CHALMERS

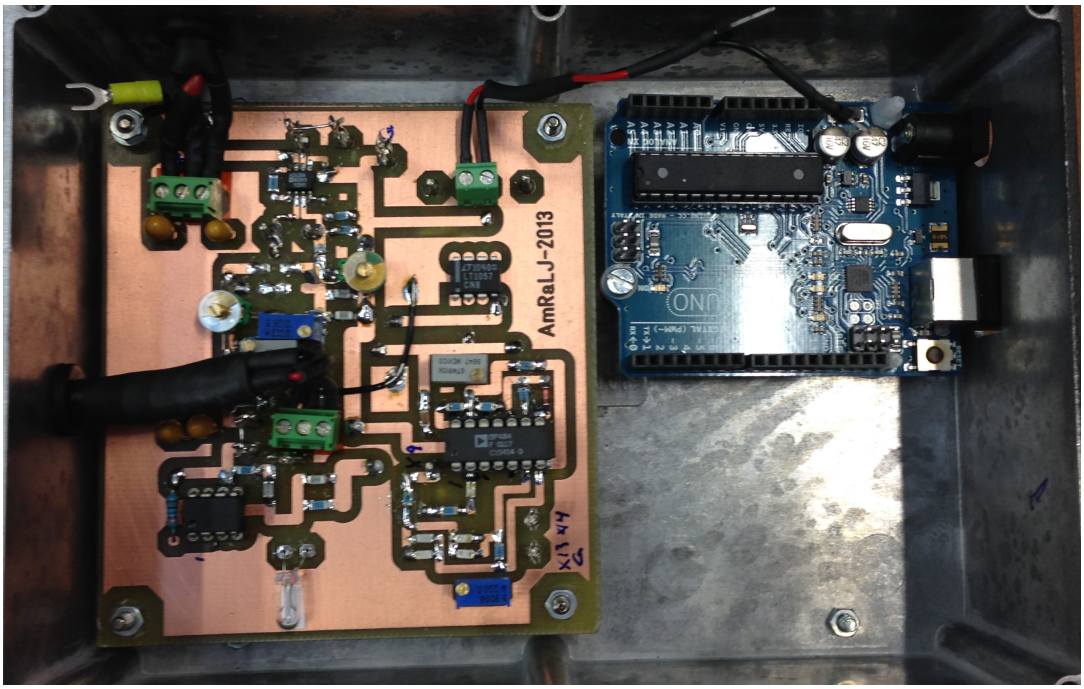

Air Content Measurement Technique

Master's Thesis in Systems, Signals and Control

RAFAEL WADIE, AHMED KACHROUDI

Department of Fluid Mechanics
CHALMERS UNIVERSITY OF TECHNOLOGY
Göteborg, Sweden 2014
Master's thesis 2013:1

Abstract

This report is a part of a Master Thesis Project in Electrical Engineering at the faculty of Fluid Mechanics at Chalmers University. The project was performed in collaboration with Volvo Group Truck Technology, one of the major leaders of truck development in the world.

The goal of this project was to design and develop a prototype that was able to detect air bubbles in the cooling system. The project started with a literature study, where several measuring techniques were investigated. The focus was on two types of measuring techniques, permittivity or resistivity. The two methods were based on measuring the capacitance or the resistance between a pair of electrodes in the coolant when air bubbles were added. Several prototypes, including various electric circuits, were developed. Between the two designs presented during the development, the capacitive method was further developed.

The result of the thesis was a cylindrical capacitive sensor tested in Volvos test rig in order to investigate how well venting of coolant in the cooling system works. As a first product in this area, the prototype was able to detect air bubbles in the test rig. Therefore, improvements are needed in order to use this product in a vehicle.

Keywords: Cooling system, Expansion tank, Capacitive sensor, Shearing-bridge, Oscillator

Acknowledgements

We would like to thank our supervisors Lars Jernqvist, Sassan Etemad at Volvo GTT and Srdjan Sasic at Chalmers University of Technology for encouragement and assistance through the thesis. We also want to thank Volvo GTT for the cooperation.

Gothenburg 2014-03-08

Contents

1
Introduction

1.1 Objektives

Modern heavy-duty truck engines with increasing specific power make the engine thermal management a challenging task. New cooling systems must be developed to cater for the increased rejected heat within limited geometrical constraints and without additional weight. This requires new solutions and innovations. To verify their function, the new components have to be simulated and tested. The expansion tank is one of the major components in the system that facilitates the de-aeration of the coolant, pressurizes the entire cooling system and acts as a reservoir for coolant. It is essential that it efficiently separate the air from the air-rich coolant that enters the tank to ensure a reliable engine cooling function

The goal of the project is to develop an electrical instrument that gives a quantitative measure of air content in the cooling system. The result of the thesis was a cylindrical capacitive sensor. The introduction aims to give the reader an understanding of the purpose of the project. It also includes a detailed description of the problem and information about the conditions for the work.

1.2 Cooling system

The main parts of the automotive cooling system are the coolant, coolant pump, engine oil cooler, thermostat, fan and the radiator. Figure 1 below illustrates the cooling system [26].

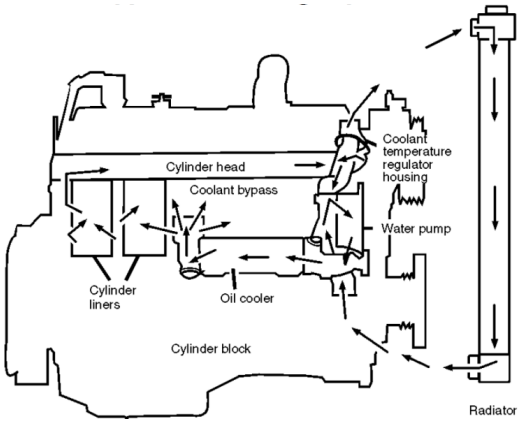

Figure 1. The cooling system [26]

The coolant pump pushes the coolant through the engine oil cooler and into the cylinder block. Thereafter, the coolant flows into the hot area of the cylinder heads. Aftercoolers, water-cooled exhaust manifolds, water-cooled turbochargers and oil coolers will transfer heat to the coolant. The coolant goes then to the thermostat.

The temperature regulators bypass the radiator and direct the coolant back to the coolant pump when the engine is cold. When the temperature regulators begins to open, the coolant will flow into the radiator as the temperature of the bypass coolant flow becomes warmer. The volume of coolant flowing to the radiator depends on the outside air temperature and the load on the engine.

Air will be pushed or pulled through the radiator by the radiator fan. The flow of air around the radiator tubes lowers the temperature of hot coolant flowing in the radiator tubes. Then, the coolant flows back through the coolant pump [26].

1.3 Expansion tank

The expansion tank is a main part of an engine's cooling system. Its main function is to allow the thermal expansion of the coolant and to separate air bubbles from the coolant and to pressurize the cooling system. When the coolant expands due to temperature changes in the cooling system, the expansion tank provides expansion volume to prevent coolant loss [26].

The expansion tank is normally placed at the top of the cooling system. This is to create a static pressure to the pump and to get better de-aeration in the system. The expansion tank size should be at least 15% of the total system coolant volume. There are built in channels in the expansion tank, forcing the liquid to move a longer distance before returning to the system via static line. Then, the air bubbles will be separated from the coolant by rising up to the surface of the expansion tank. The expansion tank needs to prevent the possibility of pump cavitation by providing a positive head on the system pump [26].

Figure 2. Expansion tank

1.4 Gas-liquid flow

According to Hewitt, Geoffrey F. the most complex form of two-phase flow is gas-liquid flows. It combine the characteristics of a deformable interface and the compressibility of one of the phases. The interfacial distribution of the gas liquid flow can take many different forms, so called flow regimes or flow patterns [21]. The flow pattern depends on the fluid properties, the flow rate of each of the flows and the size of the pipes [22]. The flows are different depending on if they occur in a vertical- or a horizontal tube.

The flow patterns in vertical flows are presented below, and illustrated in figure 3 [22,23]:

- **Bubble flow** – the gas is dispersed in the form of continues bubbles, where the liquid is continuous.
- **Slug flow** – when the concentration of bubbles becomes high, the bubbles coalesce to make larger bubbles that approach the diameter of the tube.
- **Churn flow** – the structure of the flow becomes unstable when increasing the velocity of the flow. A breakdown of the bubbles occurs leading to an oscillatory motion of the liquid upwards and downwards in the tube.
- **Annular flow** – the gas flows in the center of the tube and the liquid flows on the wall.
- **Wipsy Annular flow** – when the liquid flow rate is increased, the concentration of the gas droplets is increased, which might form large lumps or wisps of liquid.

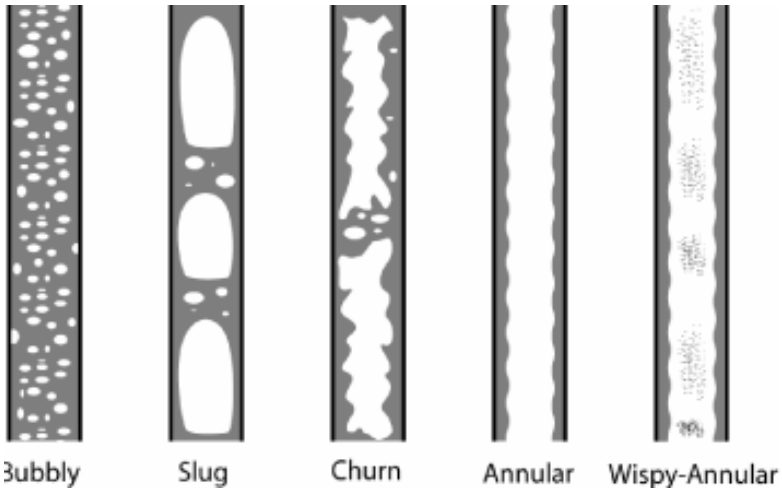

Figure 3. Flow patterns in vertical flows [24]

The two-phase flow in horizontal pipelines is almost like the one for vertical flows. A separation of the flow occurs since the gravity acts normally to the flow direction, which leads to a liquid flow on the bottom of the tube and the gas on top of it. The flow patterns in horizontal flows are presented below, and illustrated in figure 4 [22,23]:

- **Bubbly flow** – the gas bubbles are dispersed with a high concentration on the upper half of the tube due to their buoyancy. The liquid is in the lower half of the tube.
- **Stratified flow** – complete separation of the two phases occurs at low liquid and gas velocities. The liquid is in the bottom of the tube and the gas is on top.
- **Stratified wavy flow** – waves are formed on travelling in the direction of flow when increasing the gas velocity in a stratified flow.
- **Plug flow** – large bubbles are flowing near the top of the tube, the liquid is separated elongated gas bubbles. The liquid phase is continuous along the bottom of the tube. Also called **elongated bubble flow**.
- **Slug flow** – the diameter of the elongated bubbles is similar to the channel height, due to higher gas velocities. The liquid slugs contain many smaller bubbles.
- **Annular flow** – is similar to the flow pattern in vertical two-phase flow, where the gas flows in the central core and the liquid flows near the wall.

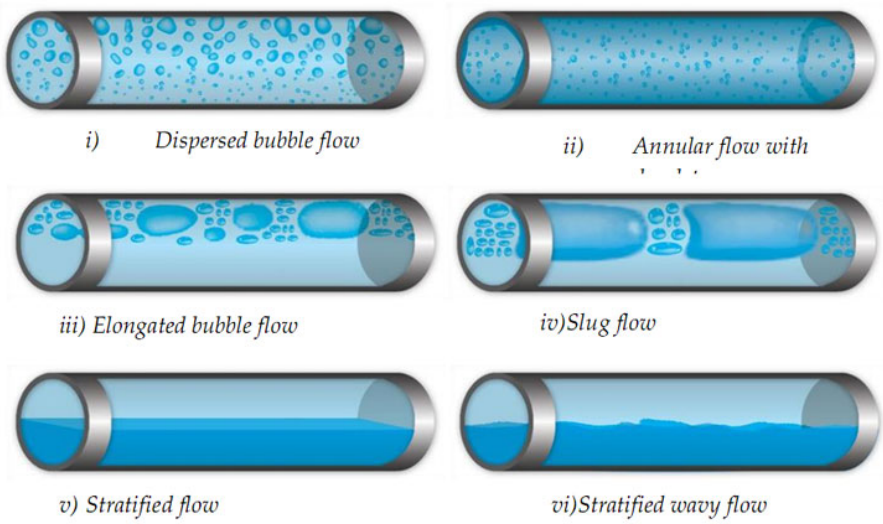

Figure 4. Flow patterns in horizontal flow [25]

2
Related work

2.1 Cavitation

Cavitation is a phenomenon based on local vaporization of a liquid. When the absolute pressure drops to a value that is equivalent to or less than the vapor pressure of the liquid at the given temperature, small bubbles of steam configuration will occur. A reduction of the pressure to a value near the vapor release the air from the liquid, as it usually is air dissolved in the liquid. The combination of air separation and vaporization is called cavitation [1].

In a flow system, the liquid becomes exposed to changes in velocity and it will affect and change the pressure. When the velocity increases, the pressure will decrease. If the pressure drops to a level low enough, cavitation may occur. Then the bubbles will flow with the fluid to a region of higher pressure, where they collapse. Cavitation contributes to noise, erosion of metal surfaces and vibrations in the system [1].

The most generally useful cavitation parameter is the cavitation coefficient:

$$\sigma = \frac{p_1 + p_c}{0.5\ \rho\ v_1^2} \qquad (1)$$

where p_1 is the static pressure, p_c it the critical pressure when cavitation occurs, ρ is the density and v_1 is the mean fluid velocity.

There are many different ways to measure cavitation. Some of the methods are the determination of NPSH (Net Positive Suction Head) at a constant speed and flow rate, measurement of the inlet flow at the impeller, measurement of static pressure in the flow system, vibration and acoustic measurement in the pump [2]. NPSH is the difference between the vapor energy and the total energy at the inlet flange of the pump [1].

2.2 Inductive measuring method

Inductive sensors use an electromagnetic field that penetrates into the target while capacitive sensor uses an electrical field for sensing the surface of the target. Inductive sensors generate an AC electromagnetic field around the end of the probe when pass an AC through a coil on the end of the probe. When this alternating field comes in contact with the target it leads to that small electric currents will be induced in the target material, which is eddy current. The closer the probe is to the target, the more eddy current probes react with the probes field and the better driver's output. [3]

The inductive sensor is affected by three parameters: the size of the probe coil and target, the distance between them and the target material. The method is used to detect cracks, flaws, weld seams and holes in the conductive material is eddy current technology. Because of its sensitivity to material changes [3]. Inductive sensors have nanometer resolution, frequency response of 80 kHz and higher, and immunity against pollution in measurement area. Usually they have the measurement range of 0.5mm-15mm.Because of their tolerance of pollution they are good choice for the environment and they work well in operation when they are immersed in a liquid [3]

Inductive sensors must be calibrated for a specific material before use because they are sensitive to different conductive target materials. Some of the materials have the same behavior; while others are have a more different behavior. There are two different types of target materials, ferrous (magnetic) and nonferrous (not magnetic). While some inductive sensors can measure both ferrous and nonferrous, others can only measure one of them. Ideally, the way you want to measure over an area that is three times as large as the probe diameter. This is because the electromagnetic field from the inductive sensor probe is approximately three times the probe diameter [3]. Examples of ferrous materials are iron and steel and for nonferruous are aluminum, zinc and copper.

Due to the fact that inductive sensors focus on metal measurement and not particles (bubbles) in the liquid, no further investigation will be made on this subject.

2.3 Permeability

In electromagnetism, permeability is the ability of the material to obtain the configuration of a magnetic field within itself. In other words, the measure of magnetization a material may have in response to an applied magnetic field [4].

Permeability is the inductance per unit length and the SI unit it is measured in Henry per meter or in Newton per ampere. The measure of the resistance when a magnetic field is created in the vacuum is the magnetic constant μ_0. The magnetic constant is $4\pi \cdot 10^{-7}$ $H \cdot m^{-1}$. The permeability for air is $1.2566375 \cdot 10^{-6}$ and for water it is $1.2566270 \cdot 10^{-6}$ [4].

The size of the permeability depends on the mediums structure and the fluid dynamic viscosity. The permeability is proportional to the flow rate and the dynamic viscosity. It

depends on a wide range of parameters, such as the frequency of the applied field, the position of the medium, temperature and humidity [4].

The properties of the medium are examined in order to calculate and separate the air bubbles from the water. The main difference in permeability constants for air and water are so small that it becomes difficult to distinguish air from water. The method is therefore not suitable for measuring the concentration of air bubbles in the liquid.

2.4 Capacitive sensors

Capacitive sensor consists of two conducting electrodes that are immersed in the liquid it acts as a capacitor. At least one of the electrodes must be insulated. The capacitance is defined as:

$$C = (A * \varepsilon_r * \varepsilon_0) / d \qquad (1)$$

where C is the capacitance in Farad, A is the area of each metal plate, ε_r is the static permittivity (the dielectric constant) of the material between the electrodes, ε_0 is the relative permittivity which is equal to 8.854×10^{-12} F/m and d is the distance between the plates [5].

The dielectric constant is a measure of the materials impact on the electric field. The capacitance is dependent on the material used as an insulator [5,6,8]. Permittivity makes it possible to store the same charge in a smaller electric field, since it relates to materials ability to transmit an electric field. A capacitor with high permittivity will have high capacitance [5].

To measure the capacitance, a capacitive sensor circuit that converts the variable plate capacitance into an output is required. The measuring circuit converts the capacitance to tension, frequency or pulse width modulation [7]. When designing a circuit for capacitance measurements, the following characteristics must be taken into account [7]:

- Good linearity, to determine the derivative
- Low noise level
- Stray electric fields and stray capacitance
- Correct choice of carrier frequency and waveshape

One of the most common capacitive sensor circuits is the analog timer circuit [6,7]. The timer circuit operates as a latch. It generates a frequency, which is determined by a

microcontroller that counts the pulses within a given period. The frequency is inversely proportional to the capacitance [7].

Another commonly used circuit for measuring the dielectric properties in capacitive sensors is the Schering-bridge. The Schering-bridge is a type of AC-bridge consisting four arms as shown in figure 1 [9].

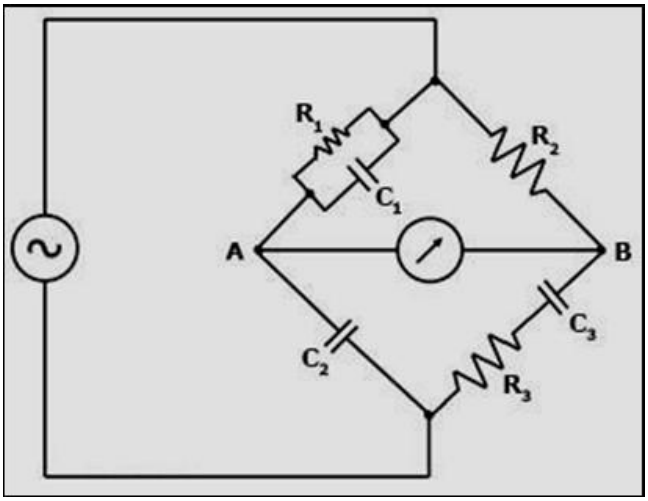

Figure 5. Schering bridge [9]

R_1, R_2, C_1 and C_2 are known. C_3 is the capacitance to be measured. R_3 is a resistance representing the loss in C_3. The bridge is in balance when the voltages at point A and B are equal. For liquid tests, cylindrical electrodes are usually connected to the Schering-bridge for the measurements [10].

2.5 Capacitive air bubble detector

Capacitive air bubble detectors have been used to detect bubbles during hemodialysis, where the detection method is capable of detecting air bubbles in the blood stream in different frequencies [11]. The capacitor is based on parallel plates capacitor with defined area and a fixed distance between the plates. The plates need to be good conductors of electricity. They should also be resistant to oxidation and corrosion at high temperatures or when exposed to chemical elements [11]. The signal from the capacitor can be carried out using RC circuit at different frequencies. To investigate if there are air bubbles in the inlet flow, the output voltage across the capacitance needs to be measured. The capacitance is calculated using equation 4:

$$C = \frac{\varepsilon_0 * \varepsilon_r * A}{d} \qquad (4)$$

where ε_0 is the permittivity of free space, ε_r is the dielectric constant of the fluid, A is the area of the metal plates and d is the separation of the plates [12].

The maximum output voltage from the capacitor can be determined by:

$$V_{CPeak} = \frac{V_{in}}{1+(2\pi fRC)^2} \quad (5)$$

where V_{CPeak} is the maximum output voltage, V_{in} is the input voltage to the RC circuit from the signal generator and f is the frequency applied on the circuit. After calculating V_{CPeak}, V_{rms} have to be determined and compared to the experimental results. The capacitance and the output voltage were measured using copper wires attached to the plates.

Abdalrahman Ahmed et al. [11,13] made an experiment about a capacitive air bubble detector operating at different frequencies for application in hemodialysis. Two platinum plates encased within an acrylic material formed a capacitor as shown in figure 6. Air bubbles in the blood stream were detected at two different frequencies, 30 Hz and 30kHz.

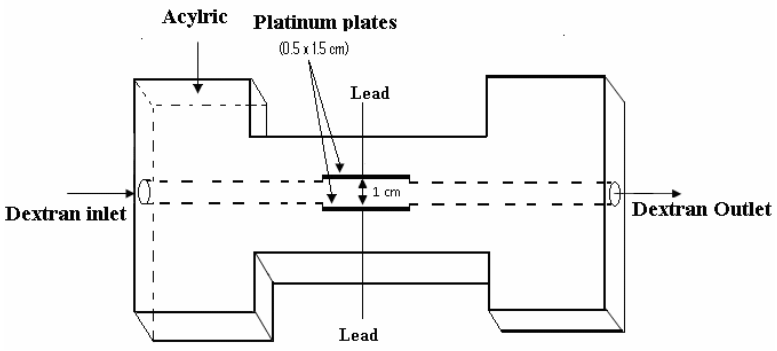

Figure 6. The capacitve detector device [11,13]

The solution used in this experiment was Dextran70, because it almost has the same density and viscosity as blood [11]. The Detxtran70 solution is first moved between the capacitor plates and then, the tubes are closed to keep the liquid in place. The capacitance and output voltage are then measured when an air bubble with given diameter was introduced in the solution.

The results from this test showed the voltage output is increases with increasing air bubble diameter. It also showed reduction in capacitance with increased air bubble diameter [11,13].

2.6 Acoustic bubble capacitor

The size of gas bubbles in liquids is relevant in petrol industry, especially when you have multiphase flow in pipelines. There are several different methods of measurements, one of them is capacitive measurement. The

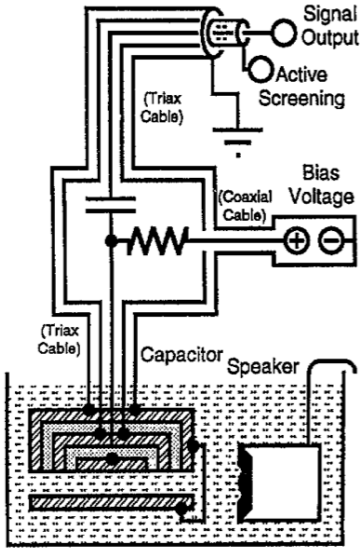

Figure 7. A schematic diagram

capacitive measurement is based on the properties of the medium where the dielectric constant of the fluid affects the capacitance value. The appearance of gas in the liquid reduces capacitance, because fluid has a higher dielectric constant than gases [14]. Another method is to use the response of the bubble to a variable frequency sound field. It is done by observing the changes of the period in the capacitance in the fluid when it is affected by a variable frequency sound field. The capacitor output signal reaches a maximum when the sound field is adapted to the natural frequency of the bubble.

The method utilized in this article uses both a capacitive measurement
and frequency response measurement, see figure 7. It is based on a variable frequency sound field which excites a bubble that is located within a capacitor. Resonance can be registered by the oscillating capacitance [14].

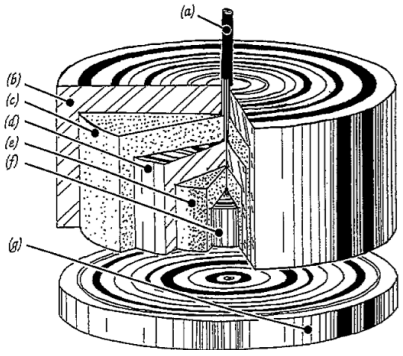

Figure 8. Bubble capacitor [14].

a) trim cable b) earthed screen c)insulator d) active

The capacitor is constructed of a circular plate surrounded by an insulating layer with the same potential as the centre of the plate, see figure 8. The bottom and the outer ring are grounded. Stray capacitance decreases due to the guard ring and the outer ring shields out the stray fields. The capacitor shielding and intermediate isolators are made of brass and nylon to reduce the noise from vibrations of the capacitor. Changes in capacitance are observed when 20-160 V is applied through a 1 GHz resistance over the plates [14].

The capacitive sensors are found to be very interesting for further investigations in this thesis. Since capacitive sensors can measure the dielectric characteristics in liquid, the properties of gas bubbles in coolant could be measured in the same way. By knowing the dielectric constant of air and coolant, the problem will be to know how gas bubbles behave in the expansion tank. A study of the distribution of gas bubbles in liquid will be made, so that we can apply an appropriate method to calculate the amount of bubbles in the coolant. Different measuring circuits should be tested.

The method in the article "The acoustic bubble capacitor: a new method for sizing gas bubbles in liquids" is based on two combined methods. The capacitive measurement method which says that appearance of gas in the liquid is reduced capacitance will be studied deeper. It has wide application area for detecting air bubbles in the fluid and a functional design.

2.7 Ultrasound

Ultrasound refers to oscillating sound wave with frequencies greater than 20kHz. In medical context, the frequency range of ultrasound is in the range of 1-20MHz [15]. Transducers made of piezoelectric crystals generate ultrasound waves. The reflection of ultrasound waves occurs at the boundary or interface of different types of tissue. The resistance to sound of the tissue is known as the acoustic impedance, and it is defined as:

$$Z = \varrho * v \quad (1)$$

where ϱ is the density of the tissue and v is the speed of sound in the tissue. To determine how much sound is reflected at the boundary of two tissue types, calculating the reflection coefficient of sound waves is defined as:

$$\alpha_r = (Z_2 - Z_1)/(Z_2 + Z_1) \quad (2)$$

where Z_1 and Z_2 are the acoustic impedance of two different tissue types. Gas bubbles reflects ultrasound signals very strongly due to the low acoustic impedance [15].

2.8 Doppler flow transducers

Doppler flow transducers consist of two piezoelectric elements placed at some angle in the direction of the flow. One of the elements transmits continues signals and the reflection is detected by the other element. Doppler flow transducers have been used in blood flow to detect gas bubbles during hyperbaric decompression [16]. The frequency of the reflecting particles in the blood is different from the transmitted signal, and the difference in frequency is proportional to the velocity of the particles. ΔF is defined as:

$$\Delta F = \frac{2 * f * v * \cos(\alpha)}{c} \quad (3)$$

where f is the frequency of the transmitted wave, v is the particle velocity, α is the angle between the incident wave and the flow, and c is the velocity of sound in the fluid.

2.9 Properties of microbubbles

There are four types of air in liquid systems. They are usually described as air pockets, gas bubbles, microbubbles and gas dissolved in the liquid. Microbubbles are hardly visible and cause a milkey looking liquid. These very small bubbles can easily follow the flow in the cooling system and if they come into contact with the solid material in the flow, the bubbles tend to grow [17].

Microbubbles are small air bubbles with a diameter up to 50 μm. Because of their small buoyancy, the rising speed of microbubbles is low. Small buoyancy and their specific area are the greatest qualities of microbubbles. Because of these qualities of the bubbles, effective resolution of gas and high absorption rate is expected. According to an approximation of the drag force by using Stokes law, the rising speed is 54 μm/s for a microbubbles with a diameter of 10 μm [17].

3

Theory

3.1 Capacitive method

After the literature study, the method that will be investigated in this project was selected. It was decided to use a capacitive sensor. The main reason for this decision is the fact that the capacitive sensor is most suitable for measuring the amount of air bubbles in the coolant.

To investigate the capability of capacitive sensor, two methods are studied. The first is based on an amplitude measure with a given fixed oscillator frequency. The second method is based on frequency measurement where the capacitance and resistance changes control the frequency.

In order to make the first measurements and test the function of the capacitive sensor a smaller test-rig was built. It allowed simpler tests and actually sees that the prototype reacted to the air change in the coolant.

3.2 Amplitude measure

To perform the basic tests for the amplitude measurements, a simple RC-circuit was built, see figure 10. The RC-circuit consists of a resistance of 1kΩ and a capacitor. A frequency generator that generates a 2 MHz signal to the RC-circuit was used. A digital oscilloscope was used to observe the amplitude differences. Since the voltage is proportional to the capacitance, observations of the amplitude gave a picture of the capacitive change. In the beginning, fixed values of the capacitors were chosen in order to compare the theoretical values to the real ones. Three different values of the capacitors (25 pF, 100 pF, 200 pF) were tested and provided the same factor size as the theoretical calculation.

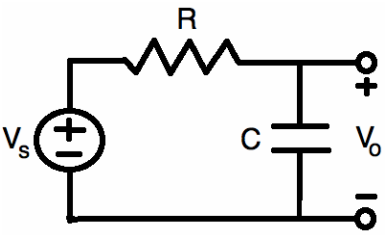

Figure 10. RC-circuit.

Several sensor configurations were studied. Thereafter, the selected fixed capacitors were replaced with two copper plates that together formed a capacitor. These plates were placed in a water bath (30cm*20cm) and were 1.5 cm apart. The size of the plates was 30 cm*1.5 cm in thickness. To investigate whether air bubbles had an influence on the capacitance, a test using different medium with similar characteristics to air was introduced. The medium was plexiglass. Plexiglass gave amplitude changes, which indicted that the RC- circuit reacted to other mediums than water.

A new configuration of plates was designed. This configuration had two outer plates, which were connected together, and one inner plate. The two outer plates should correspond to the pipe wall and the interior one corresponded to the plate between the pipes. Three tests were made, one without a water bath, one in a water bath and the last one with a water bath while the inner plate was insulated with a plastic form.

After all the necessary measurements with plate capacitors in the bath, it was time for further development of the measurement setup. The new lineup consisted of three copper plates; the new plate in the system was shorter than the previously used. The short plate was placed between the longer plates, and the two original plates were connected together and further to the RC circuit. The distance between the plates was increased from 1.6 cm to 2.6 cm.

The three plates behave as two parallel coupled capacitors. The middle plate was isolated using tape around it. The measurements were done as before, but this time the amplitude was determined in three different cases:

1. Without water or isolated middle plate
2. In water bath, but without an isolated middle plate
3. In water bath and with an isolated middle plate

The coupling scheme is presented in figure 10 and the results of the tests are shown in table 1, 2 and 3.

No water or isolated plate	
Measurement	V_{out} = 1,14V
Calculation	V_{out} = 4,44V

Table 1. Measurements and calculation without water or plate with dielectric material

Plates in water bath, no isolated plate	
Measurement	V_{out} = 36mV
Calculation	V_{out} = 119,5mV

Table 2. Capacitors in water bath, no isolated plate

Plates in water bath, one isolated plate	
Measurement	V_{out} = 102mV
Calculation	V_{out} =

Table 3. Capacitors in water bath with an isolated plate

The next measurements were done with dielectric materials between the plates. This was done by using thin overhead film and a ruler, where both materials had a dielectric constant of 3.0. The overhead film equaled 2-permille air and the ruler 10%.

3.3 Frequency measurements

A commonly used application to measure capacitive sensors is the RC-operational amplifier oscillator. The oscillator converts DC from a power supply to an AC signal. Oscillation is achieved when using positive feedback from the output of the amplifier. This type of oscillators is used when generating frequencies up to 100kHz. The output from the RC-oscillator is either a sine wave or square wave. The frequency varies depending on the change of the capacitance in the capacitive sensor.

After making some basic amplitude measurements, it was necessary to analyze the behavior of the capacitance plates connected to an oscillator. The oscillator used in this stage is called relaxation-oscillator, see figure 11. Before connecting the plates to the circuit, we used capacitors with fixed values to analyze the output frequency..

Next step was to have the capacitive plates in the water bath connected to the oscillator. The detected signal was very noisy. Therefore it was not possible to detect any changes in the signal.

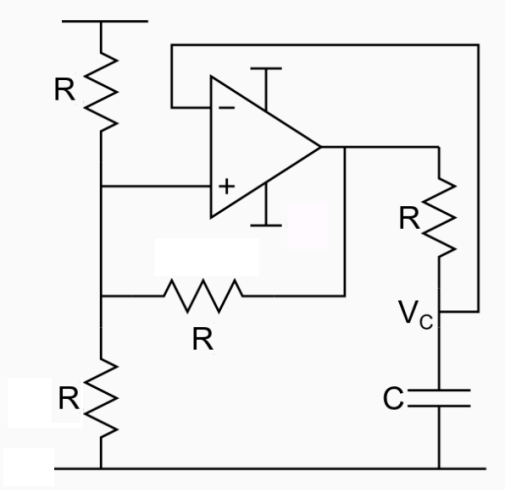

Figure 11. Relaxation oscillator.

3.4 AC bridge

The AC bridges are basic for the measurements of electrical quantities. By using an AC bridge network, measurement of capacitors and inductors can easily be performed. An AC bridge is an upgraded and improved version of a Wheatstone bridge. The Schering-bridge is a variant of AC-bridges and it is used for capacitive measurements.

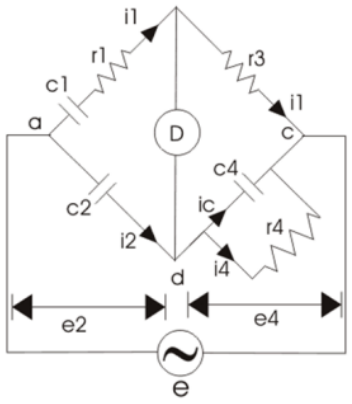

Figure 12. Schering-bridge.

3.5 Schering-bridge

A shearing bridge is used for measuring the capacitance, dissipation factor and measurements of relative permittivity. In figure 12, C_1 is the measured object and it has an unknown capacitance. C_1 is in series with the internal impedance R_1. C_2 is a regular capacitor, C_4 is a variable capacitor and R_3 is a fixed resistor. R_4 is a variable resistor and it is connected in parallel with a variable capacitor C_4. The current supply is given to the bridge between point A and C. The detector is connected between B and D.

In order to bring balance to the bridge, the theoretical value of the measuring objects (C_1) capacitance was calculated. The internal impedance (R_1) was measured using a multimeter. The inner tube of the sensor must be isolated. To verify that the isolation is good the impedance between the inner and outer tube should move toward infinity.
The supply over the bridge was chosen to +- 15 Volt.

The fixt values (measuring object) were:
$C_1 = 440$ pF
$R_1 = 5$ MΩ

After making sure that the properties of water, new coolant and used coolant gave almost identical results, new attempts to balance the bridge were made. The start frequency was 24 kHz. To find the optimal frequency, the frequency of function generator was increased with a range of about 3 kHz. The investigated frequency ranges were from 24 kHz to 100 kHz. After examining a number of factors, the optimal frequency was estimated to 84 kHz. The various factors examined were:

1. Stability of the output voltage from the bridge.
2. The sensitivity of capacitance differences when air bubbles are injected into the system.
3. How the signal behaved after ending injection of air bubbles to the system.

3.6 Coolant properties

Since it was not possible to balance the Schering-bridge with coolant in the sensor, it was necessary to investigate the properties of the coolant. The sensor was connected to a simple RC-circuit, see figure 13. It is the inner impedance (Z_x) of the sensor that will be characterized.

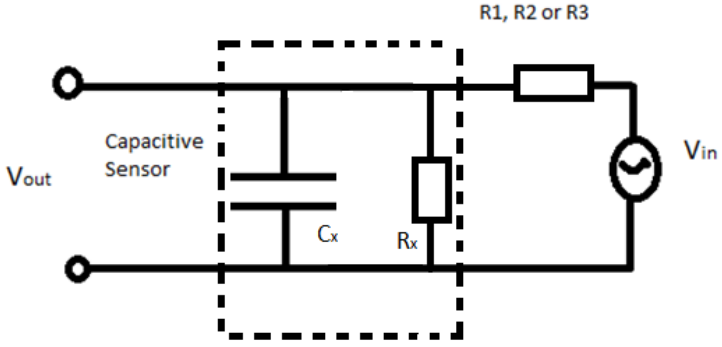

Figur 13. RC-circuit

The measurements are done as following; V_{out} is measured at a frequency where the amplitude is at maximum. Thereafter the frequency is increased until V_{out} has decreased to 71% of the start value. The new value of the frequency is the resonance frequency of the system. If the system has different resonance frequencies for water and coolant, it means that the coolant has a different dielectric constant from water.
With this type of analysis it is possible to determine R_x of the sensor when measuring with different resistors (R_1, R_2 or R_3) and liquids (water and coolant). The resistors used in the RC-circuit were 9,86kΩ (R_1), 97,7kΩ (R_2) and 0.983MΩ (R_3). V_{in} was 5V peak to peak and the starting frequency was 100Hz for the three resistors in the circuit. The flow rate was set to 6l/min. The first test was done for water, new coolant and used coolant. The results are presented in table 4, 5 and 6.

Water	
Resistance	**Frequency**
9,86kΩ	20,6kHz
97,7kΩ	1,86kHz
0.983MΩ	156Hz

Table 4. Resistance and frequency measurements for water

New Coolant	
Resistance	**Frequency**
9,86kΩ	18,2kHz
97,7kΩ	1,82kHz
0.983MΩ	159Hz

Table 5. Resistance and frequency measurements for new coolant

Used Coolant	
Resistance	**Frequency**
9,86kΩ	17,9kHz
97,7kΩ	1,84Hz
0.983MΩ	159Hz

Table 6. Resistance and frequency measurements for used coolant

The results showed that measurements with water and coolant gave almost the same resonance frequency for the sensor when measuring with different resistors. This indicated that the dielectric constant for coolant and water was almost the same.

4
Method

4.1 Design of the parallel plate capacitor

After doing the primary tests in the bridge circuit with fixed capacitors, it was necessary to design the capacitive sensor so the bridge circuit would work in the same way as when testing it on water. The fixed capacitors in the bridge were selected after the value of the plate capacitors in the bath, which had been calculated to 440pF. The sensor must have a size to fit in the test lab at Volvo. The pipes on the test rig are cylindrical, so the decision was made to use sensors with cylindrical shape. A decision was made to design two different sensors:

1. Parallel plate capacitors in a cylindrical tube
2. Cylindrical capacitive sensor

4.2 Parallel plate capacitors in a cylindrical tube

The first design contained three cupper plates in a cylindrical Plexiglas tube. The middle plate is isolated, and the plates behave as two series-connected capacitors. After determining the dimension of the plates, designs with different amounts of air and coolant between the plates were observed.
The determined parameters were as follows:

$A = 0.025*0.1m^2$
d_1 = *separation between the plates*
d_2 = *The amount of air*
d_3 = *The thickness of the insulator*
ε_1 = *dielectric constant for water = 81*
ε_2 = *dielectric constant for air = 1*
ε_3 = *dielectric constant for the insulator* ≈ 5

The separation between the plates was set to 6 cm, but it became different depending on the amount of air between the plates and the thickness of the insulator. It was assumed that the amount of air behaved as a layer between the plates. The thickness of this layer was in percent compared to the separation of the plates. As it was mentioned before, the plates behaved as two series coupled capacitors. The total capacitance of the sensor was calculated using a combination of equations 1 and 2.

$$\frac{1}{C_{tot}} = \frac{1}{C_{water}} + \frac{1}{C_{air}} + \frac{1}{C_{insulator}} \quad (1)$$

$$C = \frac{A*\varepsilon_0*\varepsilon_r}{d} \quad (2)$$

$$\frac{1}{C_{tot}} = \frac{1}{A*\varepsilon_0} * \left(\frac{d_1}{\varepsilon_1} + \frac{d_2}{\varepsilon_2} + \frac{d_3}{\varepsilon_3}\right) \quad (3)$$

Separation between plates (m)	**Thickness of air (m)**	**Amount of air (%)**	**Insulator thickness (m)**	**C_{tot} (pF)**
5.2*10^-3 m	0.7*10^-3 m	13.5 %	0.1*10^-3 m	56 pF
5.25*10^-3 m	0.65*10^-3 m	12.5 %	0.1*10^-3 m	60 pF
5.3*10^-3 m	0.6*10^-3 m	11.5 %	0.1*10^-3 m	64 pF
5.6*10^-3 m	0.3*10^-3 m	5%	0.1*10^-3 m	114 pF
5.84*10^-3 m	0.06*10^-3 m	1%	0.1*10^-3 m	292 pF

Table 7. Results for different configurations

The equations (1), (2) and (3) are valid for one parallel plate capacitor. In the end of the calculations, C_{tot} was multiplied by 2.0. The separation between the plates and the thickness of air varies due to the amount of air in the system. Table 7 shows the results for different configurations. A final calculation with clean water was made in order to investigate the difference in capacitance with and without air. The capacitance for clean water was 477 pF.

4.3 Cylindrical capacitive sensor

The cylindrical capacitive sensor consisted of one inner cupper pipe and an outer cupper cylinder. The inner pipe was isolated with teflon. The design of the cylindrical sensor was different than the one for the parallel plates. The dimensions of the pipes at the rig were measured. The pipes used in the rig had the same dimensions as the ones in the trucks installation. The second important thing was the length of the sensor. It has to be short enough to fit in a truck, but at the same time it should have a capacitance of 450-500 pF. The inner diameter of the pipes was 23mm.

The outer cupper pipe had a diameter of 20mm and a length of 160mm. The inner pipe had a diameter of 8mm and a length of 110mm. Since the capacitance is detected between the two cylinders, the active part of the sensor was about 90mm of the length of the inner cylinder, see figure 14**.**

The last part in the design of the sensor was to calculate the capacitance in the coolant. The sensor was connected to a RC circuit while immersed in coolant bath. V_{in} was set to $10V_{pk\text{-}pk}$, the frequency from the oscillator to 100khz and R = 10kΩ. V_{out} was measured to 3,14V. By using equation 4**,** the capacitance was measured to 481pF. The capacitance was within the desirable values. It resulted in further investigations with the cylindrical capacitive sensor.

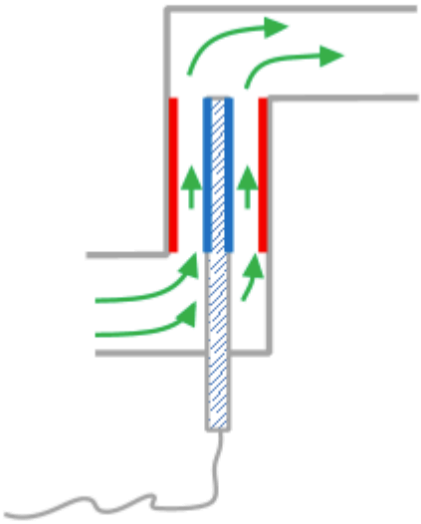

Figure 14. Cylindrical capacitive sensor

$$Vut = \frac{1}{\sqrt{1+(\omega RC)^2}} * Vin \qquad \rightarrow \qquad C = \sqrt{\frac{\left(\frac{Vin}{Vut}\right)-1}{(\omega R)^2}} \qquad (4)$$

4.4 Design of the electric circuit

In order to determine the size of the sensor, a matching electric circuit was designed. It is important to mention that the design of the circuit and sensor were done in parallel. One of the main parts of the circuit is the Schering bridge, which was already mentioned earlier in this report, see chapter 3.5. In this chapter, a brief description of each part of the circuit will be described.

4.5 Wien bride oscillator

The first part of the circuit was the Wien-bridge. It is a RC-oscillator commonly used in electric applications to replace the function generator. The Wien-bridge generates a sine wave, in which the generated resonance frequency and the voltage gain are determined. It consists of 2 capacitors, 4 resistors and an operational amplifier, see figure 15.

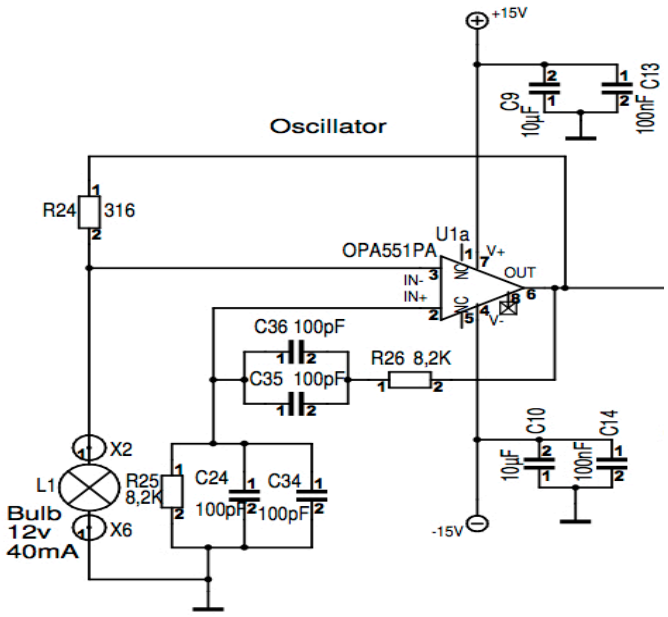

Figure 15. Wien-bridge oscillator

The negative feedback is connected via a resistor divider. One of the resistors is a lamp that limits the max current into the system. The positive feedback of the amplifier is connected to the RC network and has zero phase shift. The resonant frequency is selected in this part of the oscillator. Oscillations are caused at the selected frequency when the inverting and non-inverting inputs are equal and in-phase, so the positive feedback cancels out the negative feedback.

The generated frequency of the oscillator is by $f = \frac{1}{2\pi RC}$. In the RC-network, there are two resistors and two capacitors. This means that R_{25} is equal to R_{26} and C_{24} in parallel with C_{34} equals C_{35} in parallel with C_{36}. R_{25} and R_{26} were equal to 8,2kΩ. The use of two capacitors in parallel at each stage is because 200pF capacitors were needed, but only had 100pF. When calculating the frequency with these components, the achieved frequency will equal 97kHz. This has to do with the tolerance of the resistors and capacitors. After some experiments with different resistors and capacitors, the requested frequency (84kHz) was found using 8,2kΩ resistors and 200pF capacitors.

The gain of the amplifier can be found by $G = 1 + \frac{R_{24}}{R_{lamp}}$. The gain must be at least 3, which means that $R_{24} = 2*R_{lamp}$. R_{24} was equal to 316Ω and R_{lamp} was about 100Ω.

4.6 Band pass filter

The circuit contains two band pass filters. The first filter is an "Inverting band pass filter", see figure 16. The second one is an "Infinite gain multiple feedback active filter", see figure 17.

A simple inverting band pass filter is a combination of a first order low pass and high pass filter. The band pass filter is a filter that passes a range of frequencies while rejecting frequencies outside of the bandwidth. The frequencies inside the upper and lower limits are called pass band. The bandwidth of the filter is found by determining the minimum and maximum passing frequencies at the output stage of the amplifier [18]. F_{min} was set to be 33,8kHz, f_{max} to 159kHz and the was equal to 10.

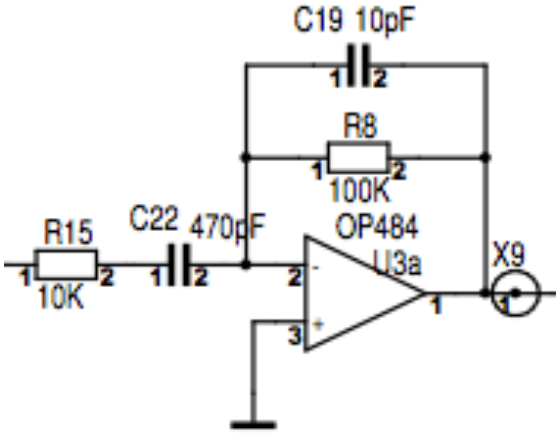

Figure 15. Simple bandpass filter

F_{min}, f_{max} and the gain are found by the following equations:

$$f_{min} = \frac{1}{2\pi * R_{15} * C_{22}}$$

where R_{15} = 10kΩ and C_{22} = 470pF → f_{min} = 33,8kHz.

The second band pass filter in the circuit was an "Infinite gain multiple feedback active filter". It uses full gain of the amplifier with multiple feedbacks applied via R_{16} and C_{28} in parallel with C_{29} as shown in figure 17**.** The relationship between R_9 and R_{16} determines the Q-factor, which is defined as the distance between the upper lower frequencies where the pass band gets narrower around f_c. The following equations are used in order to calculate the gain, the Q-factor and the center frequency of the system:

- $Maximum\ gain: G = -\frac{R_{16}}{2R_9} = -2Q^2$
- $Center\ frequency: f_c = \frac{1}{2\pi\sqrt{R_9 * R_{16} * 370pF * 370pF}}$, 370 pF is the parallel connection of the capacitors at each stage.
- $Q - factor: Q = \frac{f_c}{BW_{(3dB)}} = \frac{1}{2}\sqrt{\frac{R_{16}}{R_9}}$

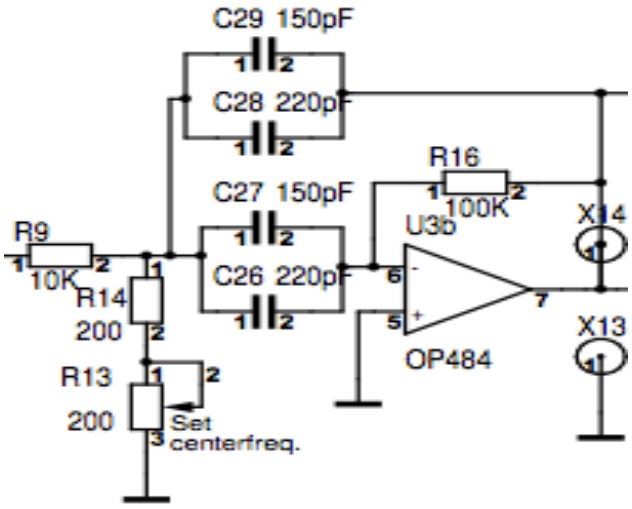

Figure 16. Infinite gain multiple feedback active filter

4.7 Full wave precision rectifier

A full wave precision rectifier is an electric circuit that converts incoming alternative current from a power source or transformer to pulsating direct current. The current that flows as a sine wave is modified so that the output current only flows in the positive direction as shown in figure 18. The circuit is shown in figure 19.

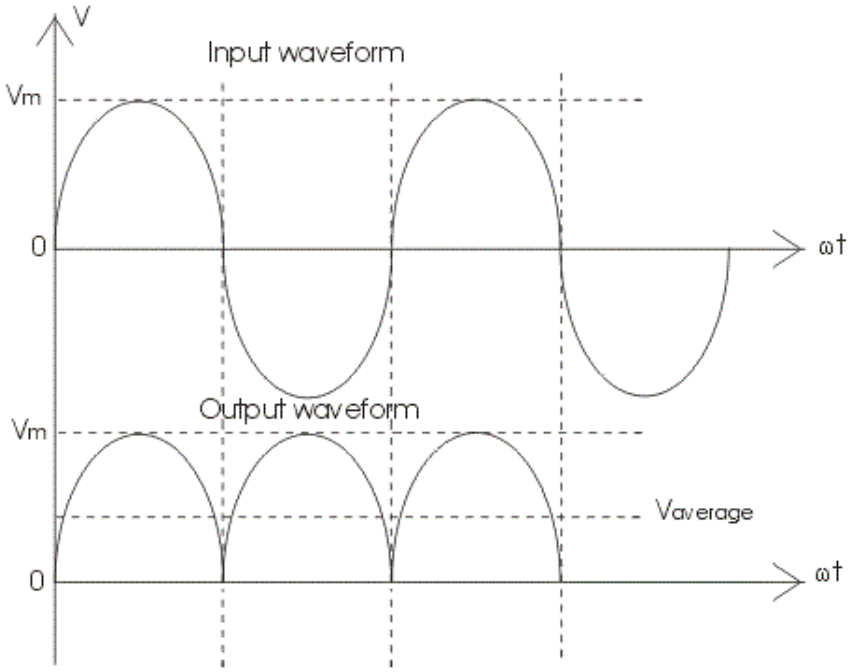

Figure 17. Rectified output

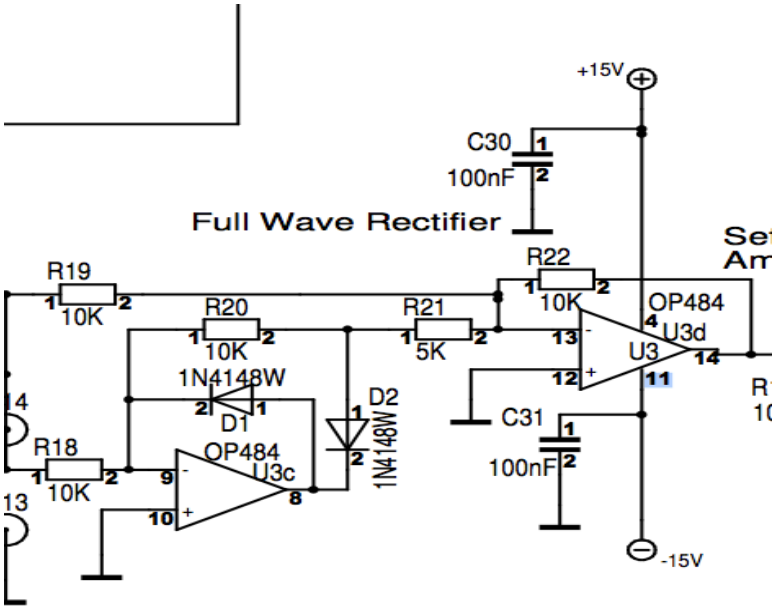

Figure 18. Full wave rectifier

The diodes are reversed to obtain a positive rectified signal. For good performance, the tolerance of the resistors should be 1% or better. The design of a full wave precision rectifier consists of two operational amplifiers and five resistors. The output of the first op-amp is negative and D_1 is reverse biased when the input signal is positive. Then, D_2 is forward biased forming an inverting amplifier by closing the feedback loop around the first op-amplifier through R_{20}. The second op-amplifier inverts the input signal, so the output will represent the absolute value of the input. This means that the output of the rectifier will always be positive [19].

4.8 Arduino

The Arduino Uno is a microcontroller board based on ATmega328, see figure 20. It consists of 14 digital input and output pins, 6 analog inputs, 16 MHz ceramic resonators, a USB connection, a power jack, an ICSP header and a reset button. Arduino is an open source platform, both hardware and software. It can receive input from different sensors and control different types of applications such as motors, lights etc [20].

The microcontroller was the last stage of the electrical circuit, and was used an AC-DC converter. It was programmed as a voltmeter, so the amount of air bubbles in the system could be readable from the computer instead of using an oscilloscope [20].

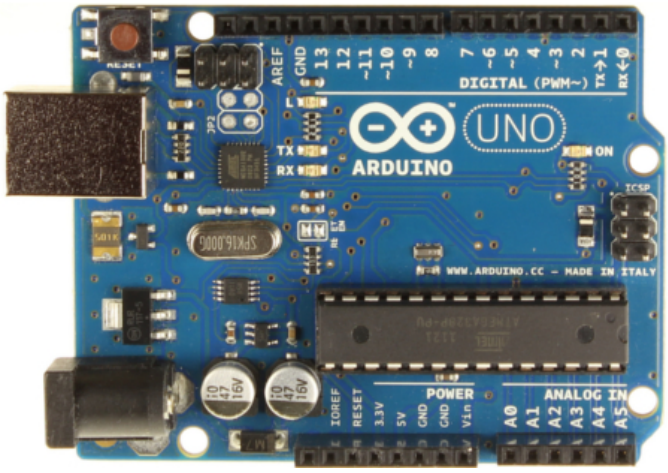

Figure 20. Aurduino Uno

5

Measurements and Results

5.1 Measurements were divided in three sections

- Calibration of the sensor
- Concentration of air-bubbles in a truck
- Concentration of air-bubbles in the rig

The measurements were done in a test rig. It consisted of:

- 2 expansion tanks
- 2 flow meters
- 1 power supply
- 1 sight glass
- Water container/tank
- Coolant pump
- Compressed air
- Connecting tubes

5.2 Calibration of the sensor

The calibration of the sensor is one of the most important parts of this project. It was done in a test rig, see flowchart1 and figure 21, where the amount of air in the system was known. The flow rate of the cooling fluid could be varied using a power supply. To determine the flow rate, there were two flow meters connected to the input stage of the sensor. Since the amount of air was known, it was possible to determine the percentage of air in the system measured by the sensor. In order to get a correct calibration, it was necessary to define were to measure the concentration of air bubbles in the system. Since the expansion tank has the task of separating air bubbles from coolant, the sensor was placed before the expansion tank in the system when calibrating it.

Before starting the calibration, it was important to vent the coolant as much as possible in order to balance the bridge circuit down to approximately zero. When the coolant had been vented and the bridge was balanced, the first measurements could be made. One of the prerequisites of the calibration was that the output signal from the sensor should be resumed to zero when there was no air in the system. Progressively, measurements with different amounts of air in the coolant were made. The calibration procedure was made three times to make sure the calibration of the sensor was stable and reliable.

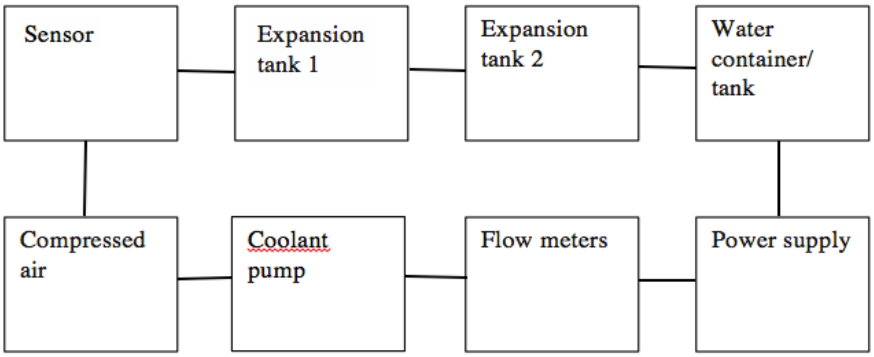

Flowchart 1. A block schedule over the calibration rig.

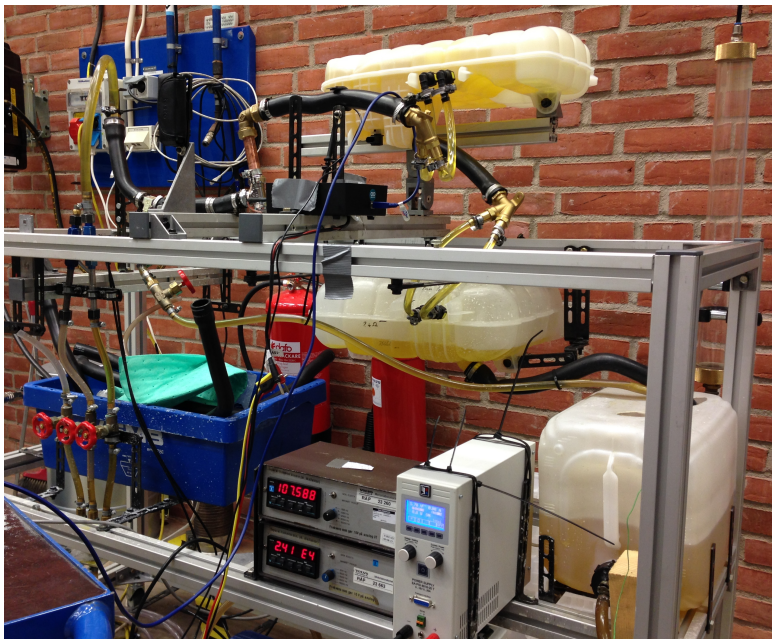

Figure 21. The rig during calibration of the sensor

The results of the calibration are presented in Graph 1. The percentage value of air bubbles in the system was determined by dividing the flow rate (liters/minute) of air with the flow rate of coolant (liters/minute). The results were plotted in Figure 22, where the x-axis is air in percent and the y-axis is the concentration of air in the system. Initially, the concentration is a voltage. Since the voltage had been amplified in many stages during the signal processing, it was not possible to set an appropriate scale due to the fact that signal was amplified. The final scale was unknown, but the unit is voltage.

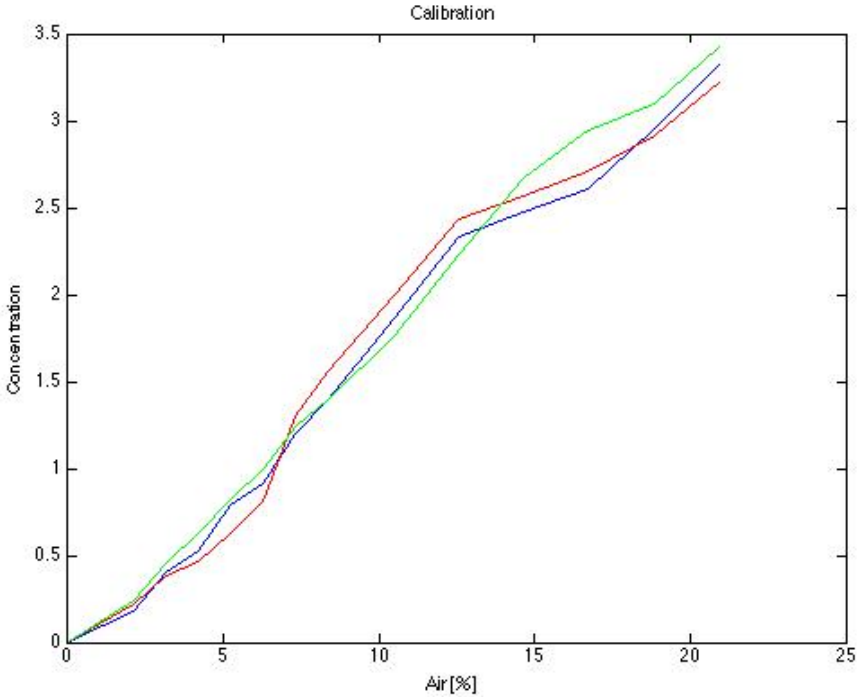

Figure 22. Three different results for calibration on rig.

5.3 Concentration of air-bubbles in a truck

The next step was to measure the concentration of air bubbles in an expansion tank in a truck, see figure 23. It was a great chance for the project to make measurements in a truck and see how the sensor would behave in real environment. There were several factors that differed between measurements in the rig and measurements in a truck. The coolant has higher temperature in the truck compared to the rig. Furthermore, vibrations caused by the truck engine can affect the behavior of air bubbles in the system. Therefore, some of the work was to examine whether these factors played an important role or not.

The measurements in the truck were made as follows:

- Before start, venting the cooling system in the truck during one hour.
- Tests to be performed when pressurizing the system to 80kPa
- Measuring the amount of air bubbles at 800, 1000, 1400, 1600 and 1800 rpm.

The sensor was placed vertically in the truck to minimize the occurrence of air pockets inside the sensor. Theoretically, there should not be any air bubbles in the system between 800-1400 rpm. Air bubbles appeared in the system at low engine speed, which made it hard to balance the bridge circuit down to zero. Furthermore, the sensor detected a lot of noise caused by the electronic around the truck and vibrations caused by the engine. A damping material was used between the electric circuit and the truck in order to reduce the vibration impact on the sensor. Unfortunately, the output signal detected a lot of noise.

The sensor was not robust during the tests in the truck. The wires between the circuit and the sensor got broke, and also the insulator got damaged. Therefore, no results were observed and no graph could be plotted.

Figure 23. Measurements in truck

5.4 Concentration of air-bubbles in the rig

The last measurements were done in the rig in order to investigate the effectiveness of separating air bubbles from coolant for different expansion tanks, see flowchart 2 and figure 24. The expansion tank was moved and placed between the input stage (coolant and air bubbles) and the sensor.

In order to get a stable value of the concentration, it was important that the injected air bubbles could be vented before injecting new air. But because of the high air pressure, small amounts of air bubbles followed in the system after closing the air pressure valve. After redesign with new valves, the system became compact without air leakage.

The next step was to start measuring the air content in the system for different percentages of air. This was done at three different times to ensure that the results were stable and credible. In the discussion section, there will be conclusions about the effectiveness of the expansion tank and how well the system separated air bubbles from the coolant, see figure 25. A brief analysis of the sensor behavior will be discussed in chapter 6.

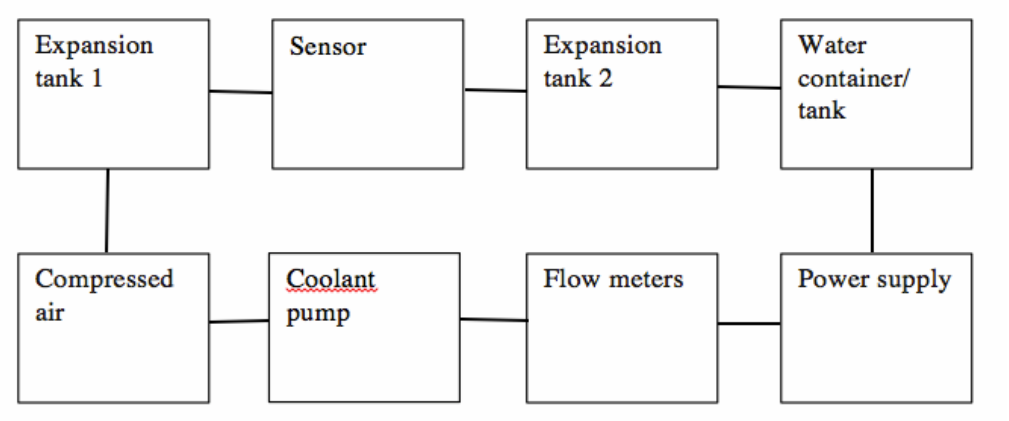

Flowchart 2. A block schedule over the rig.

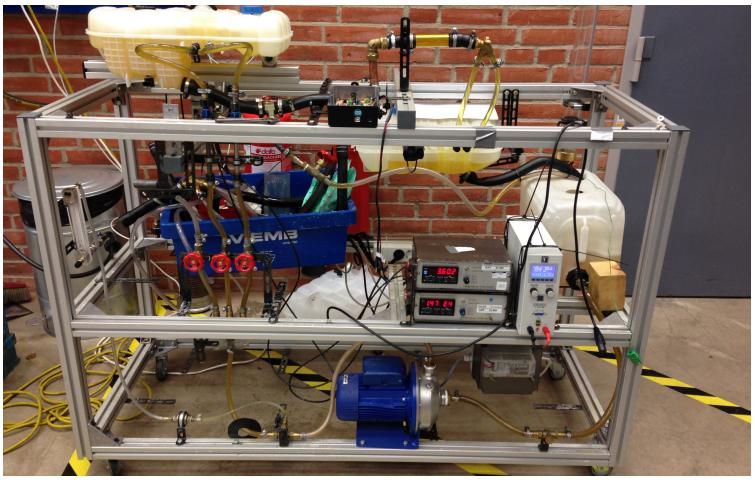

Figure 24. The rig during concentration measurements

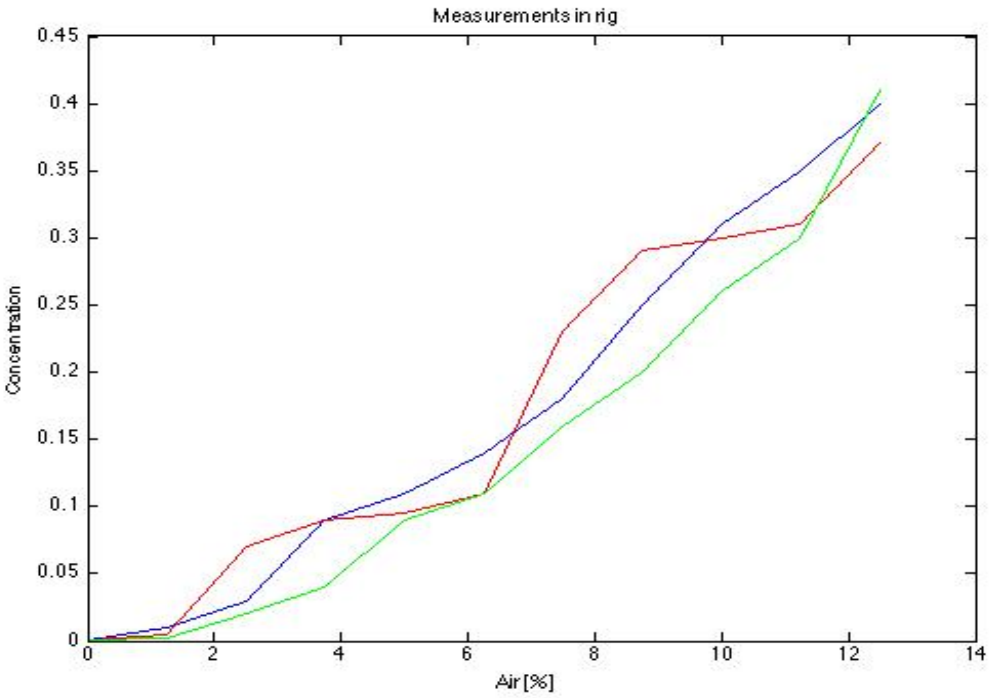

Figure 25. Measurements on rig.

6

Discussion and Future solutions

6.1 Discussion

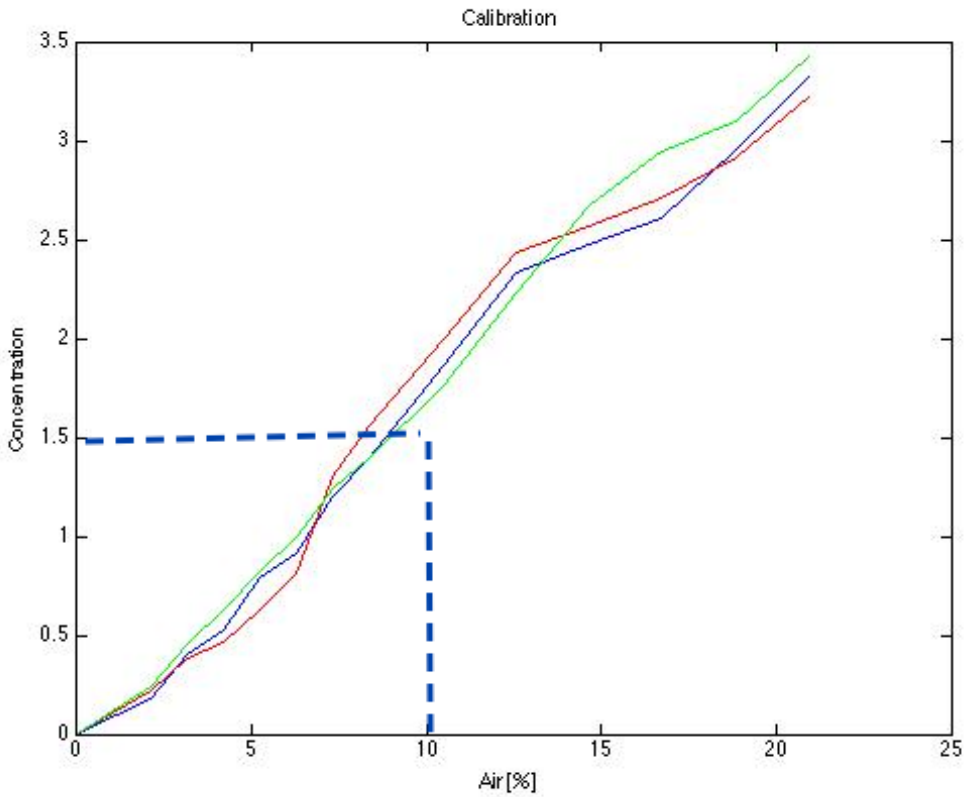

Figure 26. Calibration results. See figure 27 for comparison between the calibration and the actual measurements

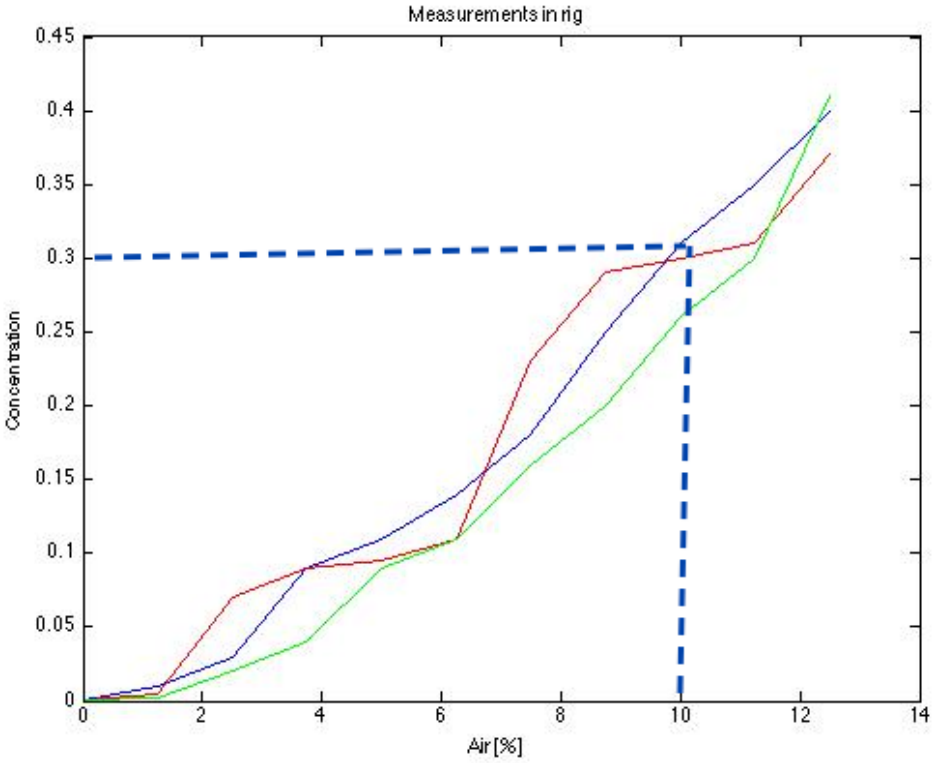

Figure 27. Measuements results. See figure 26 for comparison between the calibration and the actual measurements

The outcome of the project was to develop a prototype that was able to detect air bubbles in the coolant system. A series of measurements were made, both in rig and in a real truck. The calibration was needed in order to define the working area of the sensor. Thereafter, the results from the tests in the rig were compared with the results from the calibration. The results from the tests in the truck could not be compared with the calibration due to non-consistent results.

After evaluating the result section, it was possible to make conclusions regarding the efficiency in separating air bubbles from coolant for the expansion tank. According to figure 25, the expansion tank reduces the amount of air bubbles when it was installed before the sensor.

To compare the calibration with the real measurements, a point in the graph was chosen. The chosen point was at a concentration value of 1.5 in the calibration. It was equivalent to approximately 10% air bubbles. 10% air bubbles in the result graph represent only a concentration value of 0.3. It can therefore be concluded that the expansion tank separates air bubbles from coolant by a factor of five (1.5/0.3). It is important to note that this is based on the current prototype.

To verify if the measured value was realistic, the observation window was used to study the amount of bubbles, see figure 23 and figure 24. By looking in to the glass it was possible to determine the amount of air bubbles, whether there was an increase or decrease of air bubbles in the system. By this method it was possible to verify that a factor five in effectiveness was a logical value.

The main differences between the rig and the truck were vibrations and coolant from the truck. The coolant was heated to about 50 degrees Celsius. Because of the temperature and the harsh environment the sensor could not provide a stable concentration value. The insulator of the inner tube was damaged during the measurements, which affected the results as well. A new thicker insulator was used without much progress. The sensor showed that it was sensitive even in the truck environment and reacted to increases and decreases in air bubbles in the coolant. But still, it was hard to balance the bridge circuit and the voltage never stayed stable at 0.

6.2 Future solutions

The measurements in the truck indicated the need of further development of the sensor. In order to improve the sensor itself, suggestions of improvements are presented below.

6.2.1 Better insulator

The insulator should be thin enough not affect the detection of air bubbles in the system. By using a thin insulator, there will be less impact on capacitive properties of the sensor. It is important to use an insulator that tolerates rough environments such as high temperatures and vibrations.

6.2.2 Self balanced bridge

A self-balanced bridge would be of great benefit. The system would be self-regulated depending on the amount of air bubbles in the system. This is a proposal for a future solution that would make it easier for users. The idea is based on when the system is free from air, it shall be possible to use a "reset button" on sensor. There would not be any need of calibrating the sensor before each test.

6.2.3 Sensitivity in bridge

During the development of the sensor, the aim with the bridge circuit was to balance the output voltage down to zero for pure coolant, and detect changes in the signal when detecting air bubbles in the system. The output signal never came down to zero, but it was close enough, around 50 mV, to detect significant changes when detecting different amounts of air bubbles. Still though, the bridge circuit needs to be modified to achieve better sensitivity and an output signal to zero for pure coolant.

6.2.4 Noise filtration

During the testing and analysis of the output signal during testing in the truck, the oscilloscope detected a lot of noise. Even though we used filters in the circuit in order to remove irrelevant frequencies, the real output signal from the oscilloscope was not as expected. Therefore, better noise filtration in sensor would be demanded. The surrounding environment should not affect the sensitivity of the circuit.

6.2.5 New design ideas

Since this is the first prototype for this kind of measurements, we believe that it worked fine with good results, although it needs some improvements. The sensor was capable of detecting different amounts of air bubbles in the cooling system. The design of the sensor needs some improvements as well. By using straight inlets instead of bent ones, it will reduce the occurrence of air pockets in the sensor.

During the measurements, the output signal was affected if the wires between the circuit and the sensor were touched. The wires need to be fully screened and as short as possible. Also, a new more compact design of the sensor is preferable.

6.2.6 Conclusion

The aim of the project was to investigate whether it is possible to develop a sensor that is capable to detect air bubbles in a test bench. Since this is the first prototype for air bubble measurements in coolant system, the objective of the thesis was achieved.
Although the sensor needs some improvements, it is capable to detect different amounts of air bubbles in an expansion tank. The tests were performed in room temperature. The measurements in the truck indicated the need of further development of the sensor. A final product needs to take to account the temperature, vibrations and other electronic instruments in a real truck.

Appendix

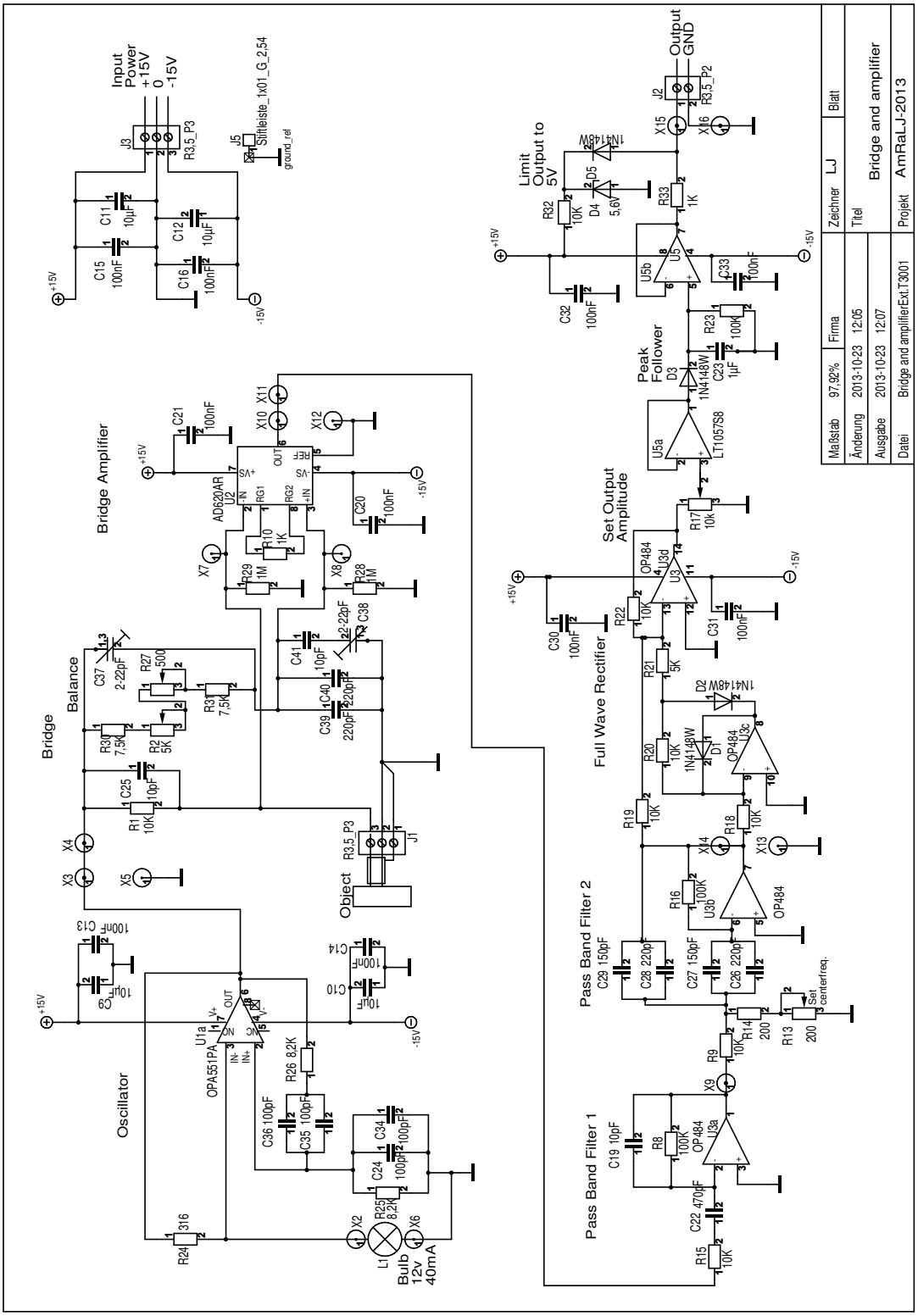

Figure 28. The design of the electic circuit

Burr-Brown Products
from Texas Instruments

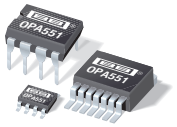

OPA551
OPA552

SBOS100A – JULY 1999 – REVISED OCTOBER 2003

High-Voltage, High-Current OPERATIONAL AMPLIFIERS

FEATURES

- **WIDE SUPPLY RANGE: ±4V to ±30V**
- **HIGH OUTPUT CURRENT: 200mA Continuous**
- **LOW NOISE: 14nV/√Hz**
- **FULLY PROTECTED:**
  Thermal Shutdown
  Output Current-Limited
- **THERMAL SHUTDOWN INDICATOR**
- **WIDE OUTPUT SWING: 2V From Rail**
- **FAST SLEW RATE:**
  OPA551: 15V/μs
  OPA552: 24V/μs
- **WIDE BANDWIDTH:**
  OPA551: 3MHz
  OPA552: 12MHz
- **PACKAGES: DIP-8, SO-8, or DDPAK-7**

APPLICATIONS

- **TELEPHONY**
- **TEST EQUIPMENT**
- **AUDIO AMPLIFIERS**
- **TRANSDUCER EXCITATION**
- **SERVO DRIVERS**

DESCRIPTION

The OPA551 and OPA552 are low cost op amps with high-voltage (60V) and high-current (200mA) capability.

The OPA551 is unity-gain stable and features high slew rate (15V/μs) and wide bandwidth (3MHz). The OPA552 is optimized for gains of 5 or greater, and offers higher speed with a slew rate of 24V/μs and a bandwidth of 12MHz. Both are suitable for telephony, audio, servo, and test applications.

These laser-trimmed, monolithic integrated circuits provide excellent low-level accuracy along with high output swing. High performance is maintained as the amplifier swings to its specified limits.

The OPA551 and OPA552 are internally protected against over-temperature conditions and current overloads. The thermal shutdown indicator "flag" provides a current output to alert the user when thermal shutdown has occurred.

The OPA551 and OPA552 are available in DIP-8 and SO-8 packages, as well as a DDPAK-7 surface-mount plastic power package. They are specified for operation over the extended industrial temperature range, –40°C to +125°C.

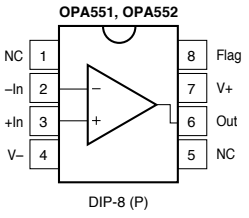

DIP-8 (P)

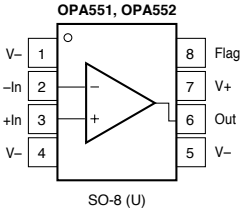

SO-8 (U)

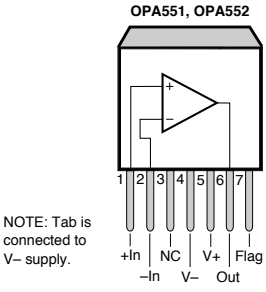

NOTE: Tab is connected to V– supply.

DDPAK-7 Surface-Mount (F)

TEXAS INSTRUMENTS
www.ti.com

Figure 29. The design of operational amplifiers, OPA551, OPA552 [27]

Precision Rail-to-Rail Input and Output Operational Amplifiers

OP184/OP284/OP484

FEATURES

Single-supply operation
Wide bandwidth: 4 MHz
Low offset voltage: 65 µV
Unity-gain stable
High slew rate: 4.0 V/µs
Low noise: 3.9 nV/√Hz

APPLICATIONS

Battery-powered instrumentation
Power supply control and protection
Telecommunications
DAC output amplifier
ADC input buffer

GENERAL DESCRIPTION

The OP184/OP284/OP484 are single, dual, and quad single-supply, 4 MHz bandwidth amplifiers featuring rail-to-rail inputs and outputs. They are guaranteed to operate from 3 V to 36 V (or ±1.5 V to ±18 V).

These amplifiers are superb for single-supply applications requiring both ac and precision dc performance. The combination of wide bandwidth, low noise, and precision makes the OP184/OP284/OP484 useful in a wide variety of applications, including filters and instrumentation.

Other applications for these amplifiers include portable telecommunications equipment, power supply control and protection, and use as amplifiers or buffers for transducers with wide output ranges. Sensors requiring a rail-to-rail input amplifier include Hall effect, piezoelectric, and resistive transducers.

The ability to swing rail-to-rail at both the input and output enables designers to build multistage filters in single-supply systems and to maintain high signal-to-noise ratios.

The OP184/OP284/OP484 are specified over the hot extended industrial temperature range of −40°C to +125°C. The single OP184 is available in 8-lead SOIC surface mount packages. The dual OP284 is available in 8-lead PDIP and SOIC surface mount packages. The quad OP484 is available in 14-lead PDIP and 14-lead, narrow-body SOIC packages.

PIN CONFIGURATIONS

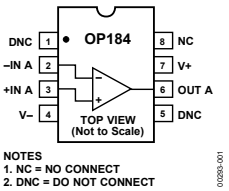

Figure 1. 8-Lead SOIC (S-Suffix)

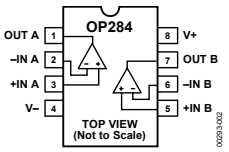

Figure 2. 8-Lead PDIP (P-Suffix)
8-Lead SOIC (S-Suffix)

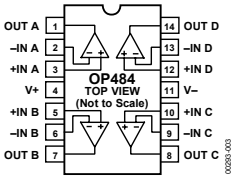

Figure 3. 14-Lead PDIP (P-Suffix)
14-Lead Narrow-Body SOIC (S-Suffix)

Table 1. Low Noise Op Amps

Voltage Noise	0.9 nV	1.1 nV	1.8 nV	2.8 nV	3.2 nV	3.8 nV	3.9 nV
Single	AD797	AD8597	ADA4004-1	AD8675/ADA4075-2	OP27	AD8671	OP184
Dual		AD8599	ADA4004-2	AD8676	OP270	AD8672	OP284
Quad			ADA4004-4		OP470	AD8674	OP484

One Technology Way, P.O. Box 9106, Norwood, MA 02062-9106, U.S.A.
Tel: 781.329.4700 **www.analog.com**
Fax: 781.461.3113

Figure 30. The design of operational amplifiers, OP184/OP284/OP484

[28]

ABSOLUTE MAXIMUM RATINGS (Note 1)

Supply Voltage ..... ±20V
Differential Input Voltage ..... ±40V
Input Voltage ..... ±20V
Output Short-Circuit Duration ..... Indefinite
Storage Temperature Range ..... –65°C to 150°C
Lead Temperature (Soldering, 10 sec) ..... 300°C

Operating Temperature Range
LT1057AM/LT1057M/
LT1058AM/LT1058M **(OBSOLETE)** ..... –55°C to 125°C
LT1057AC/LT1057C/LT1057S
LT1058AC/LT1058C/LT1058S ..... 0°C to 70°C
LT1057I/LT1058I ..... –40°C ≤ T_A ≤ 85°C

PACKAGE/ORDER INFORMATION

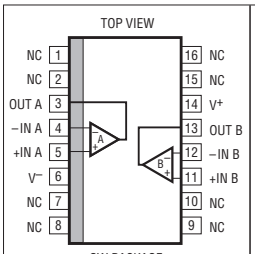

SW PACKAGE
16-LEAD PLASTIC (WIDE) SO

T_{JMAX} = 150°C, θ_{JA} = 90°C/W

ORDER PART NUMBER
LT1057SW
LT1057ISW

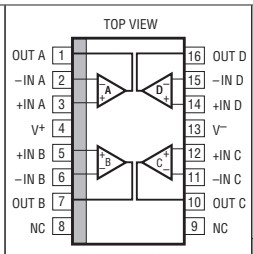

SW PACKAGE
16-LEAD PLASTIC (WIDE) SO

T_{JMAX} =150°C, θ_{JA} =90°C/W

ORDER PART NUMBER
LT1058SW
LT1058ISW

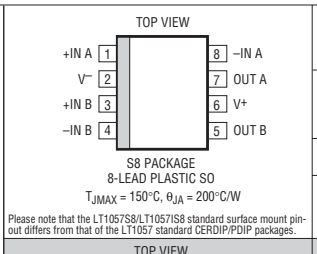

S8 PACKAGE
8-LEAD PLASTIC SO

T_{JMAX} = 150°C, θ_{JA} = 200°C/W

Please note that the LT1057S8/LT1057IS8 standard surface mount pin-out differs from that of the LT1057 standard CERDIP/PDIP packages.

ORDER PART NUMBER
LT1057S8
LT1057IS8

S8 PART MARKING
1057
1057I

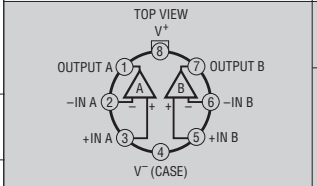

H PACKAGE 8-LEAD METAL CAN

ORDER PART NUMBER
LT1057AMH
LT1057MH
LT1057ACH
LT1057CH

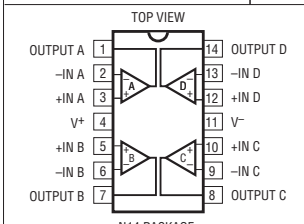

N14 PACKAGE
14-LEAD PDIP

T_{JMAX} = 125°C, θ_{JA} = 130°C/W

J14 PACKAGE 14-LEAD CERDIP
T_{JMAX} = 150°C, θ_{JA} = 100°C/W

ORDER PART NUMBER
LT1058ACN
LT1058CN
LT1058AMJ
LT1058MJ
LT1058ACJ
LT1058CJ

ORDER PART NUMBER
LT1057ACN8
LT1057CN8
LT1057ACJ8
LT1057CJ8
LT1057AMJ8
LT1057MJ8

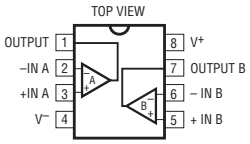

N8 PACKAGE
8-LEAD PDIP

T_{JMAX} = 125°C, θ_{JA} = 130°C/W

J8 PACKAGE 8-LEAD CERDIP
T_{JMAX} = 150°C, θ_{JA} = 100°C/W

Order Options Tape and Reel: Add #TR
Lead Free: Add #PBF Lead Free Tape and Reel: Add #TRPBF
Lead Free Part Marking: http://www.linear.com/leadfree/

Consult LTC Marketing for parts specified with wider operating temperature ranges.

Figure 31. The design of operational amplifiers, LT1057, LT1058.

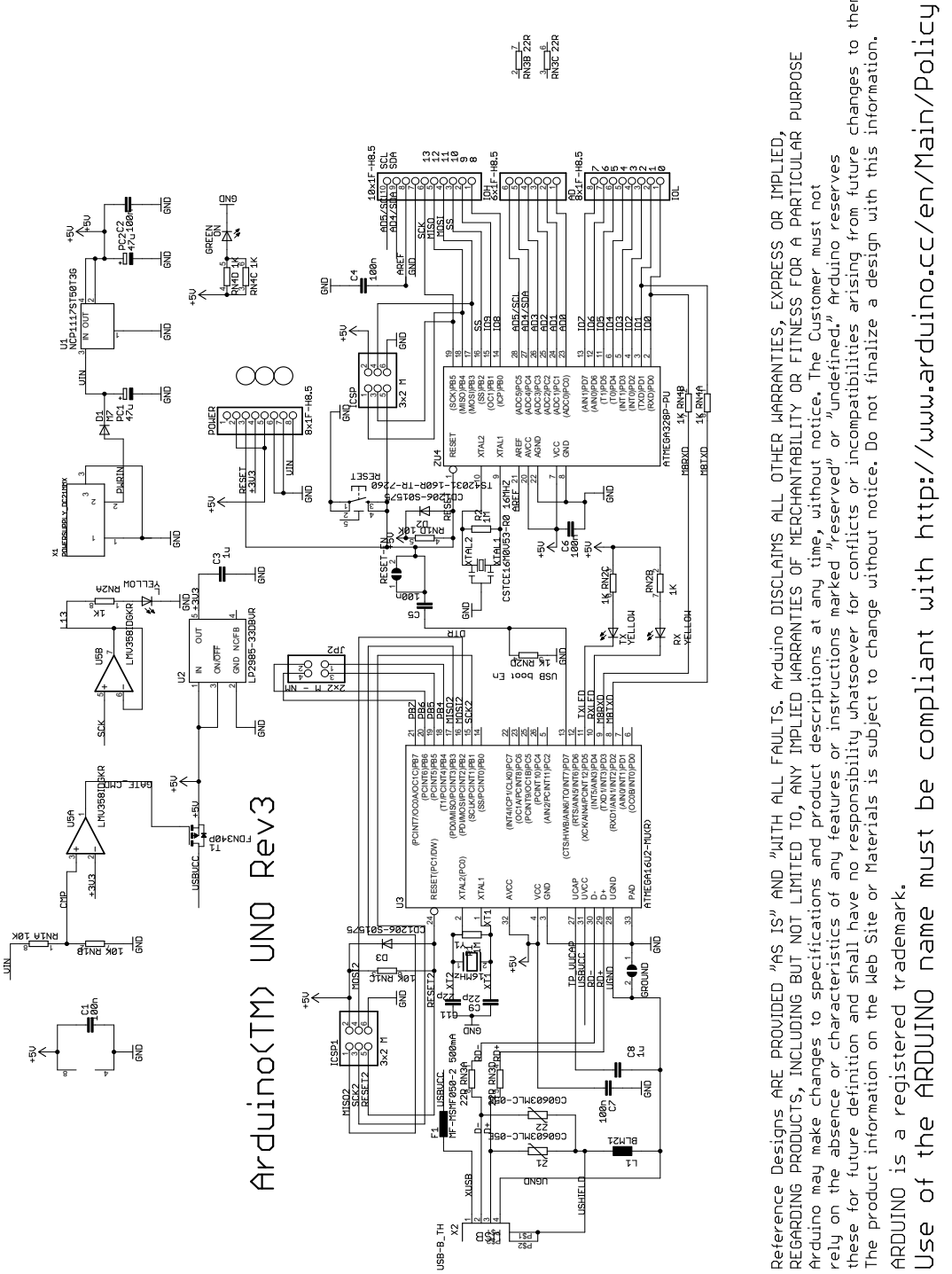

Figure 32. Arduino Uno is a microcontroller board based on ATmega328 [30]

References

[1] John F. Douglas, Janusz M. Gasiorek, John A. Swaffield, Lynne B. Jack, Fluid Mechanics, fifth edition (2005) 909-911.

[2] Jan Cernetic, Mirko Cudina, Estimating uncertainty of measurements for cavitation detection in a centrifugal pump (2011).

[3] Jon S. Wilson, Sensor Technology (2005) 196-198.

[4] http://www.ne.se/lang/permeabilitet/281996 (2013-07-02)

[5] E. Terzic et al. A Neural Network Approach to Fluid Quantity Measurement in Dynamic Environments, 2012

[6] Larry K. Baxter, Capacitive Sensors: Design and Applications, page 51.

[7] http://electronicdesign.com/analog/use-analog-techniques-measure-capacitance-capacitive-sensors (2013-06-26)

[8] http://web.mit.edu/8.02t/www/materials/StudyGuide/guide05.pdf (2013-06-25)

[9] khorshid.ut.ac.ir (2013-06-26)

[10] http://encyclopedia2.thefreedictionary.com/Dielectric+Measurements (2013-06-27)

[11] Mawahib Gafare Abdalrahman Ahmed, Abdallah Belal Adam, and John Ojur Dennis, Capacitor Device for Air Bubbles Monitoring, International Journal of Electrical & Computer Sciences IJECS Vol: 9 No: 10.

[12] Larry K. Baxter, Capacitive Sensors: Design and Applications. 48-58, 1997

[13] Mawahib Gafare Abdalrahman Ahmed, Abdallah Belal Adam, and John Ojur Dennis, Capacitive Air Bubble Detector Operated at Different Frequencies for Application in Hemodialysis, 2009.

[14] Andrew J Hardwick, Alan J Walton, The acoustic bubble capacitor: a new method for sizing gas bubbles in liquids, 1995.

[15] Ryan Dee, Looking for bubbles: Bubble detection methods for predicting decompression illness in divers, 2011.

[16] R.Y.Nishi, Ultrasonic detection of bubbles with Doppler flow transducers, 2011.

[17] Hiroaki Hasegawa, Yu Nagasaka, Hisataka Kataoka, Electrical potential of microbubble generated by shear flow in pipe with slits, 2008.

[18] http://www.electronics-tutorials.ws/filter/filter_7.html (2014-01-10)

[19] http://sound.westhost.com/appnotes/an001.htm (2014-01-18)

[20] http://arduino.cc (2014-01-21)

[21] http://www.thermopedia.com/content/2/ (2013-07-08)

[22] http://www.thermalfluidscentral.org/e-resources/download.php?id=127 (2013-07-08)

[23]http://ltcm.epfl.ch/files/content/sites/ltcm/files/shared/import/migration/COURSES/TwoPhaseFlowsAndHeatTransfer/lectures/Chapter_12.pdf (2013-07-09)

[24] http://www.scielo.br/scielo.php?pid=S1678-58782005000100004&script=sci_arttext (2013-07-10)

[25] http://www.drbratland.com/PipeFlow2/chapter1.html (2013-07-10)

[26] http://www.cat.com/cda/files/3375380/ (2013-07-19)

Appendix:

[27] http://www.mouser.com/ds/2/405/sbos100a-92760.pdf (2014-01-26)

[28] http://www.analog.com/static/imported-files/data_sheets/OP184_284_484.pdf (2014-01-26)

[29] http://cds.linear.com/docs/en/datasheet/10578fd.pdf (2014-01-26)

[30] http://arduino.cc/en/uploads/Main/Arduino_Uno_Rev3-schematic.pdf (2014-01-26)